Available online at www.sciencedirect.com

ScienceDirect

IFAC Papers Online CONFERENCE PAPER ARCHIVE

IFAC PapersOnLine 50-1 (2017) 10268–10273

Almost-Global Exponential Tracking of a Variable Pitch Quadrotor on SE(3)

Ashutosh Simha[1], Sharvaree Vadgama[1] and Soumyendu Raha[1]

Abstract: This paper presents a coordinate-free trajectory tracking control design for the nonlinear dynamics of a variable pitch quadrotor. Unlike conventional quadrotors, the rotor thrust is varied by changing its blade pitch angle as opposed to its RPM. It has been shown that such an actuation mechanism has a very high control bandwidth and is capable of producing negative thrust, which facilitates aggressive trajectory tracking. However, the control allocation in the actuator for generating the commanded thrust and torque is not a static, linear relation, but is nonlinear and dynamic. Further, transient disturbances are present due to rapid variations in aerodynamic load on the rotor dynamics while varying the blade pitch angle. The proposed control law consists of a robust attitude controller augmented with a saturated thrust-feedback position controller. The control law is shown to almost-globally stabilize the tracking errors on $SE(3)$ at an exponential rate. Numerical simulations on a model of a variable pitch quadrotor have been presented.

1. INTRODUCTION

Quadrotor UAVs have recently become popular due to their simple mechanical design and ease of control, lending themselves to educational, military and commercial applications. The quadrotor consists of two pairs of counter rotating propeller blades, located symmetrically at the vertices of a square. The propeller speeds are varied to regulate the rotor thrust, thereby generating three independent moments and a net thrust in the common direction of the rotor axes. A basic understanding of the quadrotor dynamics can be found in (Beard (2008)). Some recent applications and control designs can be found in (Lupashin et al. (2010); Hehn and D'Andrea (2011); Müller et al. (2011); Mellinger and Kumar (2011); Thomas et al. (2013); Mellinger et al. (2012)).

In conventional quadrotors, the thrust generated by each rotor is regulated by varying its speed. Such an actuation mechanism has a low control bandwidth due to saturation limits in the electro-mechanical circuit driving the rotor. Further, the rotor thrust needs to be strictly positive, thereby impairing the flight envelop. These factors have motivated the development of *variable pitch* quadrotors (Cutler (2012), Cutler and How (2012), Gupta et al. (2016)) in which rotor thrust is regulated by varying the pitch angle of the propeller blades, while maintaining a constant rotor speed. This mechanism has a significantly higher actuation bandwidth than conventional rotors. Further, the blade pitch angles can be reversed to enable negative thrust generation. While the variable pitch mechanism significantly enhances flight envelope, it however poses the following control design challenges. Unlike conventional quadrotors, the relation between the control inputs (i.e. net thrust and torques) and the blade pitch angles is nonlinear, with no closed form inverse. Hence real time control allocation requires iteratively inverting a nonlinear map which is not feasible on board. Further, when an actuator input (such as the servo motor voltage) is applied to vary the blade pitch angles, there is a rapid fluctuation in the aerodynamic load imposed on the electro-mechanical circuit driving the rotors. This leads to transient fluctuations in the rotor speed and consequently the thrust and torque coefficients.

In this paper, the nonlinear model of the variable pitch quadrotor is adopted from (Gupta et al. (2016)). The control law is designed in the following stages. First, an intrinsic geometric control law is designed on $SO(3)$ in order to (almost) globally track a commanded attitude trajectory. The control law is based on back-stepping and is distinct and more efficient than the one presented in (Lee (2013)) where bounds on structural parameters and tracking rates are imposed, which inhibit the system performance. The proposed back-stepping design is then extended to include the first order actuator dynamics whose states are the net thrust and torques about the body axes. The transients due to fluctuating aerodynamic loads as discussed above, are modeled as a bounded exogenous disturbance signal. The back-stepping design is robustified to account for the same. Finally, this control law is extended to the translational dynamics by designing a smooth saturated feedback law for the net rotor thrust which ensures (almost) globally stable tracking unlike conventional control designs (such as Lee (2013))which only guarantee local stabilization. Further, the double sided thrust generation capability has been exploited in order to design a control law which ensures that the zero equilibrium of the tracking errors is (almost) globally exponentially attractive, and is exponentially stable within the linear region of the saturation functions governing the thrust feedback. Numerical simulations with the proposed controller have been presented, where in the quadrotor initially recovers from a downward facing pose and tracks an aggressive trajectory.

[1] Department of Computational and Data Sciences, Indian Institute of Science, Bangalore-12, India

2405-8963
Peer review under responsibility of International Federation of Automatic Control.
10.1016/j.ifacol.2017.08.1476

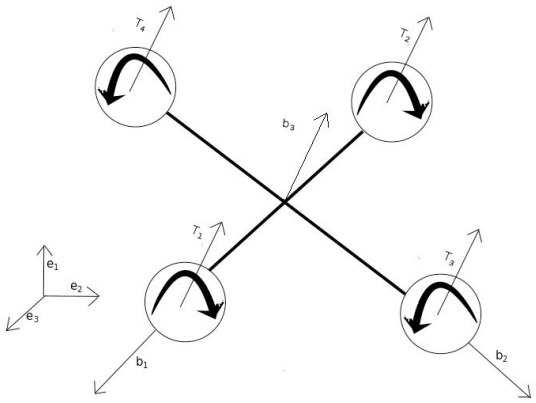

Fig. 1. Quadrotor model

2. PROBLEM FORMULATION

2.1 Quadrotor Dynamics

Consider the quadrotor as shown in Fig.1. Let $\{\boldsymbol{e}_1, \boldsymbol{e}_2, \boldsymbol{e}_3\}$ denote the inertial frame and $\{\boldsymbol{b}_1, \boldsymbol{b}_2, \boldsymbol{b}_3\}$ denote the body frame. The four identical rotors generate thrust along $\boldsymbol{b}_3$. The origin of the body frame is located at the center of mass. $R \in SO(3)$ is the rotation matrix from the $\boldsymbol{b}$ frame to $\boldsymbol{e}$ frame, denoting the attitude of the quadrotor. Ω is the angular velocity in the body frame. q and v denote the position and velocity of the center of mass. $J \in \mathbb{R}^{3\times3}$ is the inertia matrix in the body frame. f is the total thrust of the four rotors and M is the total moment in the body frame. The rigid body equations of motion are derived on $SE(3)$ i.e. the configuration manifold of the quadrotor as follows:

$$\begin{aligned} \dot{q} &= v \\ m\dot{v} &= -mge_3 + fRe_3 \\ \dot{R} &= R\hat{\Omega} \\ J\dot{\Omega} &= J\Omega \times \Omega + M, \end{aligned} \tag{1}$$

where $\hat{\cdot} : \mathbb{R}^3 \to \mathfrak{so}(3)$ is defined as $\hat{x}y = x \times y,\ x, y \in \mathbb{R}^3$. We will denote $(.)^\vee$ as its inverse map throughout the paper and e_3 as the representation of $\boldsymbol{e}_3$.

2.2 Rotor Dynamics

The thrust in each rotor is varied by changing the collective blade pitch angle of the propellers. The relation between $\Gamma = [f, M]^T$ and the thrust coefficients T_i of the rotors (in the "X" configuration) is derived using *blade element theory*(BET) along with *momentum theory* which is discussed in detail in Leishman (2002). The aerodynamic relation is derived in the nominal condition as given in Gupta et al. (2016).

$$\begin{aligned} f &= K(T_1 + T_2 + T_3 + T_4) \\ M_1 &= Kd(T_1 - T_2 - T_3 + T_4) \\ M_2 &= Kd(T_1 + T_2 - T_3 - T_4) \\ M_3 &= \sum_{i=1}^{4} (-1)^{i+1} \frac{Kr}{\sqrt{2}} \left(|T_i|^{\frac{3}{2}} + C_{D_i} \right) \end{aligned} \tag{2}$$

where $K = \rho\pi r^2\omega^2 r^2$, and $\rho,\ r,\ d, \omega$ are the density of atmosphere, radius of rotor disc, moment arm length and angular speed of the rotor and C_{D_i} are the drag coefficients of the rotor blades at zero pitch angle. The relation between T_i and the collective pitch angle for a rectangular untwisted blade can be derived using BET and momentum theory as:

$$\theta_i = \frac{6T_i}{\sigma C_{l\alpha}} + \frac{3}{2}\sqrt{\frac{|T_i|}{2}}\, sign(T_i) \tag{3}$$

where $\sigma = \frac{N_b c}{\pi r}$ is the solidity of the rotor disc, where N_b is the number of rotors, c is the chord length and $C_{l\alpha}$ is the slope of the airfoil lift curve. It can be seen that the above relation is nonlinear, with no closed form inverse. Hence (even in the nominal situation) the inverse needs to be computed onboard using an iterative scheme which is not feasible, as the attitude commands are sent at a significantly high rate. The actuator input is selected as $U = [\dot{T}_1; \dot{T}_2; \dot{T}_3; \dot{T}_4]$ which is the commanded rate of change of thrust coefficients. When the blade pitch angle is varied, there is a change in the aerodynamic load (due to increased propeller drag) on the electro-mechanical driver circuit of the rotor dynamics. Due to this, there is a transient deviation in ω from its nominal value, resulting in noisy tracking of commanded thrust and torque inputs. This phenomenon is modeled as a nonlinearly coupled disturbance in the actuator dynamics. Denote the map in (2) after factoring out ω as $\Gamma = \omega^2\Phi(T)$. The actuator dynamics is derived as:

$$\dot{\Gamma} = \omega^2 D\Phi(T)U + 2\omega\Phi(T)d(t) \tag{4}$$

where $d(t) = \dot{\omega}$ is the spurious rate of change of nominal rotor velocity, bounded as $|d(t)| < \Delta$. Denote $\sigma_1(T, \omega) = \omega^2 D\Phi(T)$ and $\sigma_2(T, \omega) = 2\omega\Phi(T)$. Equations (1) and (4) together constitute the quadrotor dynamics on $SE(3)\times\mathbb{R}^4$.

3. GEOMETRIC CONTROL DESIGN

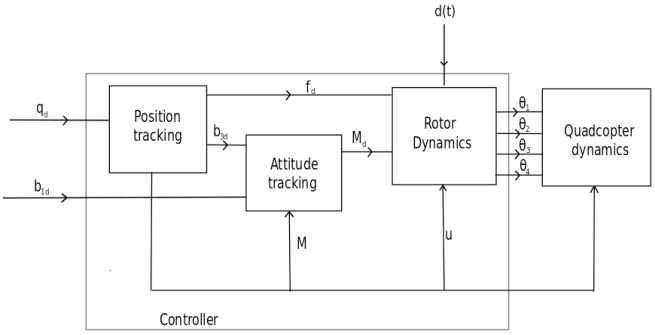

Fig. 2. Hierarchical Control Structure

The control design is carried out in two stages. First, a back-stepping based tracking control law is designed for the dynamics on $SO(3) \times \mathbb{R}^4$ for the attitude and actuator dynamics. The control objective is to track a prescribed attitude trajectory $R_d(t)$ and net thrust $f_d(t)$. In the second stage, this control law is modified to track a prescribed position trajectory on $SE(3) \times \mathbb{R}^4$. The control objective is to track the position of the center of mass along $q_d(t)$ and an appropriately prescribed heading angle.

3.1 Attitude Tracking Control Design

We now derive a back-stepping controller for the attitude dynamics on $SO(3)$. We prescribe an attitude trajectory

$R_d(t)$, and net thrust f_d. A feedback control law is derived for the actuator input U.

Let $\Psi(R, R_d) = \frac{1}{2}Tr[I - R_d^T R]$ be a tracking error function on $SO(3)$ (Bullo (2005)). It can be seen that $\Psi \in [0, 2]$. Its derivative is obtained as

$$\begin{aligned}\dot{\Psi} &= -\frac{1}{2}Tr[R_d^T R\hat{\Omega} - \hat{\Omega}_d R_d^T R] \\ &= -\frac{1}{2}Tr[R_d^T R(\hat{\Omega} - R^T R_d \hat{\Omega}_d R_d^T R)] = e_R^T e_\Omega\end{aligned} \tag{5}$$

where $e_R = \frac{1}{2}(R_D^T R - R^T)^\vee$, $e_\Omega = \Omega - R^T R_d \Omega_d$ and Ω_d is the angular spin corresponding to R_d. We use the relation: $-\frac{1}{2}Tr[\hat{x}\hat{y}] = x^T y$ and, $Tr[xs] = Tr[\frac{1}{2}(x - x^T)s]$ $\forall x \in M(n, \mathbb{R}),\ s \in \mathfrak{so}(3)$.

The second term in e_Ω is obtained from the parallel transport of the angular velocity in the tangent space at R_d to the tangent space at R. Denote

$$e_{\Omega_d} = -K_R e_R,\ K_R > 0 \tag{6}$$

It can be seen that $\Psi(t) \to 0$ asymptotically (in fact exponentially) when $e_\Omega = e_{\Omega_d}$ and $\Psi(0) < 2$. We denote the derivative of e_{Ω_d} which is affine in e_Ω as

$$\dot{e}_{\Omega_d} := C(R, R_d)e_\Omega \tag{7}$$

Denote $\tilde{e}_\Omega = e_\Omega - e_{\Omega_d}$. With this, a desired feedback torque to track R_d asymptotically is chosen using the back-stepping procedure as,

$$\begin{aligned}M_d = &-J\Omega \times \Omega + J(R^T R_d \dot{\Omega}_d - \hat{\Omega} R^T R_d \Omega_d) \\ &+JC(R, R_d)\,\mathrm{e}_\Omega - \alpha e_R - K_\Omega \tilde{e}_\Omega\end{aligned} \tag{8}$$

where $K_\Omega,\ \alpha > 0$.

Denote $\Gamma_d = [f_d; M_d]$ and $\tilde{\Gamma} = \Gamma - \Gamma_d$. The back-stepping procedure is extended to the rotor dynamics to derive a robust control law for U as,

$$U = \sigma_1(\omega, T)^{-1}\left(\frac{\tilde{\Gamma}}{||\tilde{\Gamma}||}||\sigma_2(\omega, T)||\Delta - K_a\tilde{\Gamma} - [\tilde{e}_\Omega, 0]^T\right) \tag{9}$$

Proposition 3.1. With the choice of control law U as given in (9), the attitude and actuator errors $e_R, \tilde{e}_\Omega, \tilde{\Gamma}$ are almost globally exponentially stable. Further, if the initial conditions satisfy: $\Psi(R(0), R_d(0)) = \varphi < 2$ and

$$[C_1]:\quad \frac{\lambda_{max}(J)}{2}||\tilde{e}_\Omega(0)||^2 + ||\tilde{\Gamma}(0)||^2 < \alpha(2 - \varphi) \tag{10}$$

then $\Psi(t) < 2\ \forall t > 0$ and $\Psi(t) \to 0$ asymptotically

Proof Consider a Lyapunov function for the attitude and actuator dynamics as

$$V_a = \alpha\Psi(R, R_d) + \frac{1}{2}\tilde{e}_\Omega^T J\tilde{e}_\Omega + \frac{1}{2}\tilde{\Gamma}^T\tilde{\Gamma} \tag{11}$$

Using the control law (9), its derivative is obtained as

$$\begin{aligned}\dot{V}_a = &-K_R||e_R||^2 - K_\Omega||\tilde{e}_\Omega||^2 - K_a||\tilde{\Gamma}||^2 \\ &-(||\tilde{\Gamma}||||\sigma_2(\omega, T)||\Delta - \tilde{\Gamma}^T\sigma_2(\omega, T)d(t))\end{aligned} \tag{12}$$

It can be seen that the last term is negative semi definite using the Cauchy Schwartz and matrix norm inequality. Hence

$$\dot{V}_a \leq -Z_a^T W Z_a \tag{13}$$

where $Z_a = [||e_R||; ||\tilde{e}_\Omega||; ||\tilde{\Gamma}||]$ and $W = \begin{bmatrix}K_R & 0 & 0\\ 0 & K_\Omega & 0\\ 0 & 0 & K_a\end{bmatrix}$.

This ensures that V_a monotonically decreases and condition [C1] ensures that the sub-level set $\Psi^{-1}[0, 2)$ is positively invariant. This can be seen from the fact that

$$\alpha\Psi(R(t), R_d(t)) \leq V_a(t) \leq V_a(0) < 2\alpha \tag{14}$$

Further, the first term in V_a can be bounded between two quadratic forms as

$$\frac{1}{8}||e_R||^2 \leq \Psi \leq \frac{1}{4(2 - \varphi)}||e_R||^2 \tag{15}$$

(Note: The relation state above is the corrected version of the erroneous one stated in Lee et al. (2010) and Lee (2013)). Therefore, V_a can be bounded as

$$Z_a^T M_1 Z_a \leq V_a \leq Z_a^T M_2 Z_a \tag{16}$$

where

$$M_1 = \frac{1}{8}\begin{bmatrix}\alpha & 0 & 0\\ 0 & 4\lambda_{min}(J) & 0\\ 0 & 0 & 4\end{bmatrix}\ and\ M_2 = \frac{1}{8}\begin{bmatrix}\frac{2\alpha}{(2-\varphi)} & 0 & 0\\ 0 & 4\lambda_{min}(J) & 0\\ 0 & 0 & 4\end{bmatrix} \tag{17}$$

From (13) and (16) it can be seen that the tracking error Z_a is exponentially stable and

$$\dot{V}_a \leq -\left(\frac{\lambda_{min}(W)}{\lambda_{max}(M_2)}\right)V_a \tag{18}$$

Finally, (14) ensures that $\Psi(R, R_d) \to 0$ asymptotically for all initial conditions in an open dense set. □

3.2 Position Tracking Control Design

In this section, the back-stepping control law is extended to the translation dynamics, to derive a saturation based feedback law for the net thrust, in order to (almost) globally exponentially track a prescribed trajectory $q_d(t)$ of the center of mass. We begin by denoting the position and velocity errors as $e_x = q - q_d$, $e_v = v - \dot{q_d}$. We now design a saturation based feedback law for the net rotor thrust.

Definition: Given constants a and b such that $0 < a \leq b$, a function $\sigma : \mathbb{R} \to \mathbb{R}$ is said to be a smooth linear saturation function with limits (a, b), if it is smooth and satisfies:

(1) $s\sigma(s) > 0,\ \forall s \neq 0$
(2) $\sigma(s) = s,\ \forall |s| \leq a$
(3) $|\sigma(s)| \leq b,\ \forall s \in \mathbb{R}$

Let σ_1 and σ_2 be two saturation functions with limits (a_1, b_1) and (a_2, b_2) such that,

$$b_1 < \frac{a_2}{2}. \tag{19}$$

We now define a control law for $\hat{f}$ which is the total vector thrust acting on the rigid body, as follows:

$$\hat{f} = \bar{\sigma}(e_x, e_v) + m\ddot{q}_d + mge_3 \tag{20}$$

where

$$\bar{\sigma}(e_x, e_v) = -\begin{bmatrix} \sigma_2\left(\frac{k_1}{k_2}e_{v_1} + \sigma_1\left(k_2 m e_{v_1} + k_1 e_{x_1}\right)\right) \\ \sigma_2\left(\frac{k_1}{k_2}e_{v_2} + \sigma_1\left(k_2 m e_{v_2} + k_1 e_{x_2}\right)\right) \\ \sigma_2\left(\frac{k_1}{k_2}e_{v_3} + \sigma_1\left(k_2 m e_{v_3} + k_1 e_{x_4}\right)\right) \end{bmatrix}, \tag{21}$$

and $k_1,\ k_2$ are positive constants.

From this, f_d and R_d are chosen as follows.

$$b_{3_d} = R_d e_3 = \left\{ \begin{array}{l} \frac{\hat{f}}{||\hat{f}||} \ : \ \hat{f}(0)^T R(0) e_3 > 0, \\ -\frac{\hat{f}}{||\hat{f}||} \ : \ \hat{f}(0)^T R(0) e_3 < 0 \end{array} \right\} \tag{22}$$

and,

$$f_d = \hat{f}^T R e_3 \tag{23}$$

Note that the limits of the saturation functions can be appropriately chosen to ensure that $||\hat{f}$ does not vanish, and the above quantities are well defined.

The choice for f_d and b_{3_d} is motivated by the fact that at $t = 0$ for almost all initial conditions, either $\boldsymbol{b}_3$ or $-\boldsymbol{b}_3$, is within a cosine angle of 90° with respect to $\hat{f}(0)$. This ensures that the attitude error can always be initialized to be within the region of exponential stabilization on $SE(3)$. In conventional quadrotors, there is an initial phase before the dynamics enter this region, in which there could be significant transient growth in translational errors. The above choice of f_d and b_{3_d} is made possible due to the negative thrust generation capability of variable pitch rotors. It would not have been possible in the case of a conventional quadrotor. Equation (22) represents two choices of convention for tracking i.e., the positive body z axis with positive thrust or the negative one with negative thrust. It will be shown subsequently that the sublevel set $\Psi^{-1}[0, 1)$ is positively invariant, which implies that this convention once chosen, need not be altered.

A relative heading angle trajectory $\hat{b}_{1_d}(t)$ is chosen in the plane perpendicular to b_{3_d}. Having done so, the desired attitude trajectory is given as follows:

$$\begin{array}{l} b_{2_d} = \frac{b_{3_d} \times \hat{b}_{1_d}}{||b_{3_d} \times \hat{b}_{1_d}||}, \ R_d(t) = [b_{1_d}, b_{2_d}, b_{3_d}] \\ b_{1_d} = \frac{b_{2_d} \times b_{3_d}}{||b_{3_d} \times b_{2_d}||} \end{array} \tag{24}$$

We choose the feedback law for U as

$$U = \sigma_1^{-1}\left(\frac{\tilde{\Gamma}}{||\tilde{\Gamma}||}||\sigma_2||\Delta - K_a\tilde{\Gamma} - [\tilde{e}_\Omega; (m e_v^T + c_1 e_x^T) R e_3]\right) \tag{25}$$

where the terms involved are as defined earlier, and f_d and R_d are as defined in (23) and (24).

Proposition 3.2. Define the following quantities:

$$W_1 = \begin{bmatrix} \frac{ck_x}{m}(1 - \sin(\theta_0)) & -\frac{ck_v}{2m}(1 + \sin(\theta_0)) \\ -\frac{ck_v}{2m}(1 + \sin(\theta_0)) & k_v(1 - \sin(\theta_0)) - c, \end{bmatrix},$$

$$W_2 = \begin{bmatrix} (c/m) f_M & 0 & 0 \\ a_1 + f_M & 0 & 0 \end{bmatrix},$$

$$f_M = \sup_{t>0} ||m\ddot{q}_d(t) + mge_3||_2. \tag{26}$$

Given $0 < k_x := k_1$, $0 < k_v := (k_1/k_2) + k_2$, and $\theta_0 := \arccos(b_{3_d}(0), R(0)e_3) < \pi/2$, we choose positive constants c, K_R, K_Ω, such that

$$\begin{array}{l} c < min\Big\{ k_x k_v (1 - \sin(\theta_0))^2 \Big(k_x(1 - \sin(\theta_0)) \\ + \frac{k_v^2 (1 + \sin(\theta_0))^2}{4m} \Big)^{-1}, k_v(1 - \sin(\theta_0)), \sqrt{k_x/m} \Big\}, \\ min\ (\alpha k_q, k_\Omega) > \frac{4||W_2||^2}{\lambda_{min}(W_1)}. \end{array} \tag{27}$$

Then, with the choice of the control law (25), the origin of the tracking errors $e_R,\ e_\Omega,\ e_x,\ e_v$ is exponentially attractive for all initial conditions satisfying condition [C1]

Proof Following the proof of proposition 3.1, the sublevel set $\Psi^{-1}[0, 1)$ is positively invariant after a finite time, for all initial conditions satisfying [C1], for any given trajectory $q_d(t)$. Consider the Lyapunov function for the point mass translation dynamics

$$V_b = \frac{1}{2}k_x||e_x||^2 + \frac{1}{2}m||e_v||^2 + c_1 e_x^T e_v \tag{28}$$

Following the proof of *Theorem 3.5* in (Simha et al. (2017)), we conclude that the closed loop flow of the dynamics enters the linear region of the saturation functions σ_1 and σ_2 after a finite time, after which the following can be established:

Let $Z_b = [||e_x||, ||e_v||]$. Then,

$$\dot{V}_b|_{f=f_d} \leq -Z_b^T W_1 Z_b - Z_b^T W_{12} Z_a \tag{29}$$

Consider a Lyapunov function for the complete dynamics as $V = V_a + V_b$. Using (16), we can bound V by the following quadratic forms

$$Z_a^T M_1 Z_a + Z_b^T M_3 Z_b \leq V \leq Z_a^T M_2 Z_a + Z_b^T M_4 Z_b \tag{30}$$

where

$$M_3 = \frac{1}{2}\begin{bmatrix} k_x & -c \\ -c & m \end{bmatrix},\ M_4 = \frac{1}{2}\begin{bmatrix} k_x & c \\ c & m \end{bmatrix} \tag{31}$$

and M_1 and M_2 are as defined in (16). On applying the back-stepping control law (25), the derivative of the Lyapunov function along the closed loop trajectories on $SE(3)$ and the actuator state space is obtained on the lines of (13) as

$$\dot{V} \leq \dot{V}_b|_{f=f_d} - Z_a^T W Z_a = -Z_b^T W_1 Z_b - Z_b^T W_{12} Z_a - Z_a^T W Z_a \tag{32}$$

Further the conditions of the proposition ensure that the matrices $M_1,\ M_2,\ M_3,\ M_4,\ W,\ W_1,\ W_2,\ W_{12}$ are positive definite and $\dot{V}$ is a negative definite quadratic form. Hence, the tracking errors defined in $Z_a,\ Z_b$ are exponentially

stable. Finally, since $\Psi^{-1}[0,1)$ is positively invariant, $\Psi \to 0$ asymptotically. $\square$

An important distinction from existing control designs on $SE(3)$ is that the stability analysis is global. The saturated thrust feedback was essential in enabling such analysis. Conventional linear feedback laws fail to ensure global stability, and require the translational errors to be restricted to a local region.

4. NUMERICAL SIMULATIONS

The parameters of the quadrotor chosen for simulation are $m = 2kg,\ r = 0.18m,\ c = 0.03m,\ d = 0.3m,\ C_{l\alpha} = 5.23,\ N_b = 2,\ \omega = 650rad/s.$

The nominal inertia parameters for control design were chosen as $J = diag([0.0810, 0.0812, 0.132])$.

The actual inertia matrix was perturbed as

$$J_a = \begin{bmatrix} 0.0972 & 0.0194 & 0.0195 \\ 0.0194 & 0.0974 & 0.0317 \\ 0.0195 & 0.0317 & 0.1584 \end{bmatrix} \tag{33}$$

A helical trajectory was chosen as

$$q_d = 4[sin(t); cos(t); 10 + t]. \tag{34}$$

The relative heading angle was prescribed to be constant at 0° i.e. $\hat{b}_{1_d} = [1; 0; 0]$. The initial conditions prior to tracking the helical trajectory were chosen as

$$R(0) = \begin{bmatrix} 1.0000 & 0 & 0 \\ 0 & \cos(170^\circ) & -\sin(170^\circ) \\ 0 & \sin(170^\circ) & \cos(170^\circ) \end{bmatrix} \tag{35}$$

$\Omega(0) = 0$, $q(0) = [5; 5; 5]$, $v(0) = 0$. The estimated bound on the disturbance was chosen as $\Delta = 0.5$. The control gains employed were $k_x = 2,\ k_v = 3,\ K_R = K_\Omega = diag([0.5, 0.5, 0.1]), \alpha = 1$. Fig.3 shows the center of mass

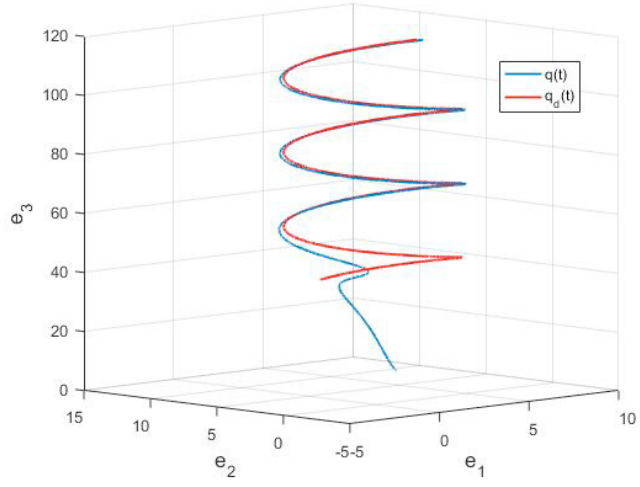

Fig. 3. Helical trajectory tracking with constant heading angle

tracking a helical trajectory with a constant relative reference heading angle, and Fig.4 shows the corresponding position errors. It can be seen that the tracking errors are sufficiently bounded despite disturbances in the rotor dynamics. This is due to the robustifying component int the control law.

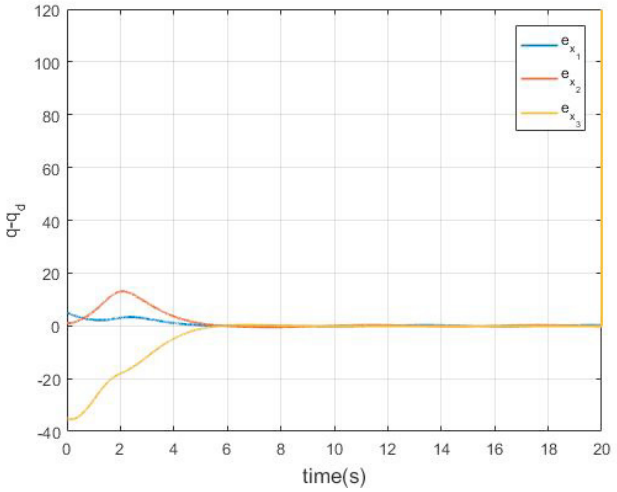

Fig. 4. Position error e_x during Helical maneuver

Fig.5 shows the variation in the error function Ψ during the maneuver. As indicated, quadrotor initially has a downward facing attitude from which it recovers. Fig.7 shows the variation in the angular velocity during the maneuver.

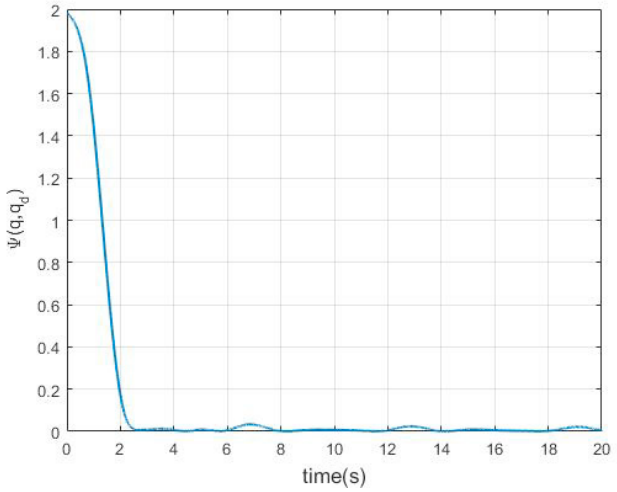

Fig. 5. Attitude error $\Psi(R, R_d)$ during helical maneuver

Fig.6 shows the variation of rotor thrusts during the maneuver. It can be seen that the rotor thrust is initially negative, which ensures exponential trajectory tracking. This would not have been possible in case of a conventional quadrotor where the rotor thrust is constrained to be strictly positive. There, the quadrotor would initially propel downwards until the attitude has recovered. This could lead to large transients in the translational errors, which may be fatal in case of a near ground maneuver.

5. CONCLUSION

A geometric backstepping control law was developed on $SE(3) \times \mathbb{R}^4$ for tracking an arbitrarily prescribed center of mass trajectory and an appropriately prescribed heading angle. An important distinction of the proposed control law over existing geometric controllers on $SE(3)$ is that

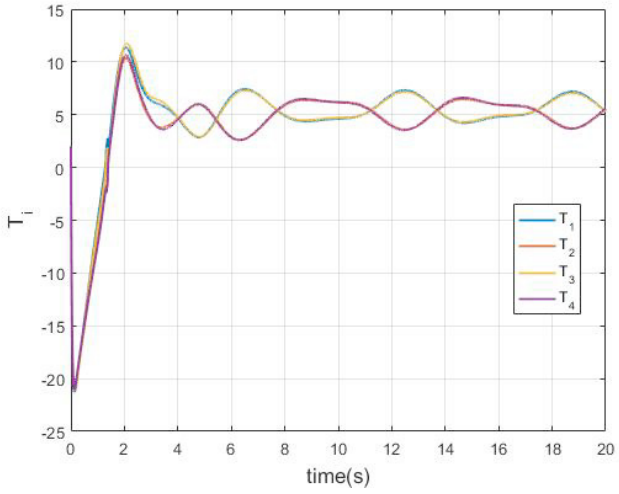

Fig. 6. Variation of rotor thrusts T_i during helical manuever

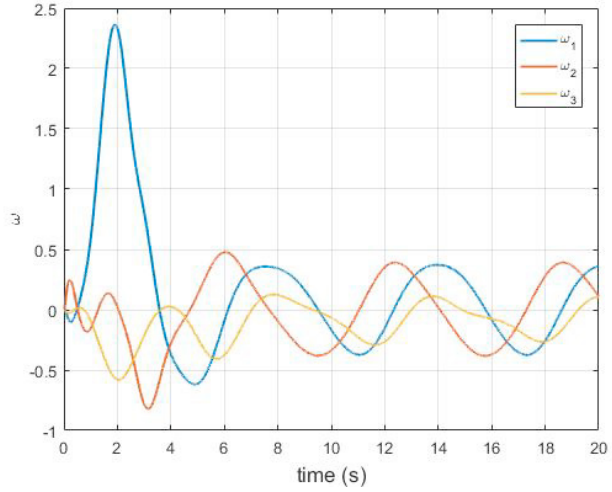

Fig. 7. Variation of angular velocity Ω during helical manuever

the saturated thrust feedback enabled (almost) global stabilization of tracking errors, at an exponential rate, unlike the former case where the stability is only local. The backstepping control law was robustified to account for nonlinearly coupled transient disturbances in the actuator dynamics due to the varying aerodynamic load, thereby rendering the control design practically applicable. The quadrotor was made to track a nontrivial trajectory in which the coefficients of thrust were seen take both positive and negative values. Such trajectories for a similar conventional quadrotor may have been impossible to track. An important avenue for further research is to refine the aerodynamic model of the variable pitch rotors, especially during translational flight and aerobatic maneuvers, and subsequently refine the control design.

6. ACKNOWLEDGEMENT

The author would like to thank Dr. Mangal Kothari, Department of Aerospace Engineering, IIT Kanpur for valuable information regarding the design of the variable pitch mechanism and related aerodynamics.

REFERENCES

Beard, R. (2008). Quadrotor dynamics and control rev 0.1.

Bullo, F. (2005). *Geometric control of mechanical systems*, volume 49. Springer Science & Business Media.

Cutler, M. and How, J.P. (2012). Actuator constrained trajectory generation and control for variable-pitch quadrotors. In *AIAA Guidance, Navigation, and Control Conference*, 1–15.

Cutler, M.J. (2012). *Design and control of an autonomous variable-pitch quadrotor helicopter*. Ph.D. thesis, Citeseer.

Gupta, N., Kothari, M., et al. (2016). Flight dynamics and nonlinear control design for variable-pitch quadrotors. In *American Control Conference (ACC), 2016*, 3150–3155. American Automatic Control Council (AACC).

Hehn, M. and D'Andrea, R. (2011). A flying inverted pendulum. In *Robotics and Automation (ICRA), 2011 IEEE International Conference on*, 763–770. IEEE.

Lee, T. (2013). Robust adaptive attitude tracking on with an application to a quadrotor uav. *IEEE Transactions on Control Systems Technology*, 21(5), 1924–1930.

Lee, T., Leok, M., and McClamroch, N.H. (2010). Geometric tracking control of a quadrotor uav on se (3). In *Decision and Control (CDC), 2010 49th IEEE Conference on*, 5420–5425. IEEE.

Leishman, J.G. (2002). Challenges in modeling the unsteady aerodynamics of wind turbines. In *ASME 2002 Wind Energy Symposium*, 141–167. American Society of Mechanical Engineers.

Lupashin, S., Schöllig, A., Sherback, M., and D'Andrea, R. (2010). A simple learning strategy for high-speed quadrocopter multi-flips. In *Robotics and Automation (ICRA), 2010 IEEE International Conference on*, 1642–1648. IEEE.

Mellinger, D. and Kumar, V. (2011). Minimum snap trajectory generation and control for quadrotors. In *Robotics and Automation (ICRA), 2011 IEEE International Conference on*, 2520–2525. IEEE.

Mellinger, D., Michael, N., and Kumar, V. (2012). Trajectory generation and control for precise aggressive maneuvers with quadrotors. *The International Journal of Robotics Research*, 0278364911434236.

Müller, M., Lupashin, S., and D'Andrea, R. (2011). Quadrocopter ball juggling. In *Intelligent Robots and Systems (IROS), 2011 IEEE/RSJ International Conference on*, 5113–5120. IEEE.

Simha, A., Vadgama, S., and Raha, S. (2017). A geometric approach to rotor failure tolerant trajectory tracking control design for a quadrotor. *arXiv preprint arXiv:1704.00327v1*.

Thomas, J., Polin, J., Sreenath, K., and Kumar, V. (2013). Avian-inspired grasping for quadrotor micro uavs. In *ASME 2013 International Design Engineering Technical Conferences and Computers and Information in Engineering Conference*, V06AT07A014–V06AT07A014. American Society of Mechanical Engineers.